JOURNAL OF MATERIALS SCIENCE 28 (1993) 6622–6630

Characterization of the pyrolytic conversion of polysilsesquioxanes to silicon oxycarbides

F. I. HURWITZ, P. HEIMANN, S. C. FARMER
NASA Lewis Research Center, Cleveland, OH 44135, USA

D. M. HEMBREE Jr
Oak Ridge Y-12 Plant, Martin Marietta Energy Systems Inc., Oak Ridge, TN 37831, USA

A series of silsesquioxane copolymers synthesized by hydrolysis and condensation of phenyl- and methyltrimethoxysilanes have been studied as preceramic polymers. The pyrolytic conversion to ceramics was characterized by thermogravimetric analysis, ^{29}Si and ^{13}C nuclear magnetic resonance and Raman spectroscopy. The pyrolysed materials were further characterized by differential thermal analysis, X-ray diffractometry and transmission electron microscopy. The ratio of phenyl to methyl groups in the copolymer was found to control polymer structure and rheology, as well as ceramic composition and char yield. On pyrolysis to 1000 °C under inert conditions, silicon oxycarbides were formed, along with glassy carbon. On heating from 1200 °C to 1400 °C, the oxycarbide structure diminished, and the materials were comprised primarily of amorphous silica, amorphous Si–C, some small crystallite SiC and graphitic carbon. The carbon content increased, and char yield decreased, with increasing concentration of phenyl groups in the copolymer. The presence of free carbon appears to inhibit the crystallization of silica. Significant carbothermal reduction was observed only above 1500 °C. Oxidation studies of the pyrolysed materials indicated the presence of at least two forms of carbon.

1. Introduction

Silicon oxycarbides, in which silicon, oxygen and carbon are incorporated into an amorphous network structure have been reported by a growing number of researchers. They are shown to remain stable over a range of temperatures, and may or may not contain amorphous carbon as a separate phase. Homeny *et al.* [1] postulated the formation of oxycarbide on incorporation of carbon at levels of 0.5–2.5 wt % in the Mg–Al–Si–O–C system, based on increases in Young's modulus, shear modulus, Vickers hardness and fracture toughness with increasing carbon content. Oxycarbide phases also have been reported at the SiC/SiO_2 interface as a metastable layer upon oxidation of SiC at temperatures of < 1250 °C, as characterized by infrared and X-ray photoelectron spectroscopy (XPS) [2].

Evidence for silicon oxycarbides in polycarbosilane-derived materials, including the polycarbosilane-derived Nicalon fibre, have been presented [3–8], primarily on the basis of X-ray photoelectron spectroscopy (XPS) and ^{29}Si nuclear magnetic resonance (NMR), which delineates tetrahedral $SiC_{4-x}O_x$ species. Raman spectroscopy confirms the presence of free carbon in polycarbosilane-derived ceramics [8, 9]. Above 1200 °C, CO and SiO are evolved [9, 10], most probably by decomposition of the metastable silicon oxycarbide, and, in the case of Nicalon fibre, the degradation is characterized by crystallization of the fibre and accompanying loss of fibre strength [11].

A number of siloxane-derived silicon oxycarbides also have been reported [12–16]. These contain substantially more oxygen than do the polycarbosilane derived materials, and depending on the particular polymer system, begin to crystallize between 1300 and 1400 °C. This group of materials has potential application as ceramic composite matrices and as coatings and sealants for high-temperature materials. The actual upper-use temperature of these silicon oxycarbides in an oxidizing atmosphere remains undefined, but may depend upon the structure of the particular oxycarbide and the quantity and distribution of any included free carbon.

Zhang and Pantano [13] studied a group of oxycarbides synthesized from alkyltrimethoxysilanes, and found that the amount of carbon incorporated into the oxycarbide was independent of alkyl chain length. They did note, however, that substantially more carbon could be incorporated into the pyrolysed materials if phenyltrimethoxysilane was the starting monomer. The oxycarbides were characterized to pyrolysis temperatures of 1000 °C.

Control of carbon content could be expected to influence the thermal expansion, modulus and perhaps oxidative stability of the pyrolysed product. The present work focuses on systematically varying copolymer composition to control the carbon content of the resulting amorphous materials, as well as characterizing the influence of polymer composition and structure on the pyrolytic conversion process.

0022–2461

Methyl- and phenyltrimethoxysilane were employed as monomers. Pyrolysis was carried out in an inert atmosphere to temperatures of 1400 °C.

Polymers were characterized by Fourier transform–infrared spectroscopy (FTIR) and nuclear magnetic resonance (NMR). The conversion process and intermediate and final products were characterized by thermogravimetric analysis (TGA), differential thermal analysis (DTA), coupled TGA/FTIR, X-ray diffraction, Raman spectroscopy, ^{13}C and ^{29}Si solid-state NMR, transmission electron microscopy (TEM) and elemental analysis.

2. Experimental procedure

Polysilsesquioxanes of the general formula $RSiO_{1.5}$ were synthesized from methyltrimethoxy- and phenyltrimethoxysilanes by hydrolysis/condensation in acid solution at pH 3.0, as described elsewhere [16]. Polymethylsilsesquioxane, polyphenylsilsesquioxane, and methyl/phenyl copolymers having various monomer feed ratios, were prepared.

FTIR spectra of polymer samples were obtained from films cast from acetonitrile on to polished KBr discs. All spectra were obtained using a Perkin–Elmer Model 1750 (Perkin–Elmer, Norwalk, CT) Fourier transform infrared spectrometer at a resolution of 2 cm^{-1}.

^{29}Si NMR of polymer samples were determined in acetone-d6 solution using a Bruker AM-300 spectrometer. Tetramethylsilane (TMS) was used as a reference. Chromium acetylacetonate ($Cr(acac)_3$) was added to the solution as a relaxation agent.

Thermogravimetric analysis was conducted in flowing argon (30 $cm^3\,min^{-1}$) at a heating rate of 10 °C min^{-1} using a Perkin–Elmer TGA 7.

Analysis of gases evolved during the early stages of pyrolysis were obtained using a Bio-Rad FTS 40 interfaced with an Stanton Redcroft TGA 1000 (Bio-Rad, Cambridge, MA). Spectra were collected at 8 cm^{-1} resolution coadding 16 scans per spectrum. Samples were heated from 35 to 1000 °C at a rate of 20 °C min.

Elemental analysis of the pyrolysed materials was performed by Galbraith Laboratories (Knoxville, TN). Carbon was determined by combustion in oxygen using an induction furnace technique. Silicon was measured by sodium fusion and ICP analysis. Oxygen was obtained by difference.

Samples for Raman spectroscopy were prepared by pyrolysis of starting polymers in a tube furnace in flowing argon. Chunks of the pyrolysed material were embedded in an epoxy mounting material and polished to a 0.5 μm finish using diamond pastes. The Raman data were obtained with an Instruments S.A. Ramanor U1000 spectrometer equipped with a Nachet microscope (Instruments S.A., Edison, NJ). The samples were imaged and the laser was focused using a Leitz NPL 100 × (0.9) objective (Ernst Leitz, Wetzlar, Germany). The 514.5 nm line from a Coherent Innova 90-5 argon ion laser (Coherent, Inc., Palo Alto, CA) was used as the excitation source in all cases.

Samples for DTA, solid-state NMR, and X-ray diffractometry were crushed using a boron carbide mortar and pestle. Differential thermal analysis was performed in both flowing argon and air (30 $cm^3\,min^{-1}$) using a Perkin–Elmer DTA 1700. X-ray diffraction patterns were recorded with a Scintag X-ray diffractometer using CuK_α radiation. Both ^{29}Si and ^{13}C MAS–NMR spectra were obtained on an AM-300 Bruker spectrometer using a pulse width of 2.5 s and a relaxation delay of 60 s.

Specimens for TEM were characterized as ion-milled foils prepared from bulk material by standard techniques of grinding, polishing and dimpling to thicknesses less than 40 μm. Material was then ion milled at 6 kV to perforation. Specimens were examined using a Phillips 400T transmission microscope equipped with a Kevex ultrathin window detector for energy dispersive spectroscopy.

3. Results and discussion

The polysilsesquioxanes all showed infrared spectra (Fig. 1) characterized by a broad Si–O–Si absorption in the 1130–1000 cm^{-1} region, and by a sharper and overlapping peak at 1134 cm^{-1} which increased in intensity with phenyl content. The presence of silanol groups in all polymers was evidenced by an Si–OH peak at 900 cm^{-1} and a broad OH stretching band at 3400 cm^{-1}. $Si–C_6H_5$ bending peaks were observed at 1595 and 1431 cm^{-1}; the $Si–CH_3$ bending is seen at 1273 cm^{-1}.

The ratio of phenyl to methyl infrared absorbances increased with phenyl content, but in a non-linear manner (Fig. 2), suggesting a change in polymer backbone structure at phenyl compositions of 60%–70%. This is consistent with an increase in linear backbone structure and decrease in branching seen in the NMR with increasing phenyl content (Fig. 3).

TGA traces of the polymers heated in flowing argon are shown in Fig. 4. The first step in the weight loss begins almost immediately on heating, with the maximum rate of loss occurring at 103–110 °C. This is attributed to evolution of free water, as well as continued condensation of silanol and methoxide groups, and is confirmed by the disappearance of the Si–OH bending and OH stretching peaks in the infrared, as well as by the presence of water and methanol in the TGA/FTIR characterization of evolved gases. An

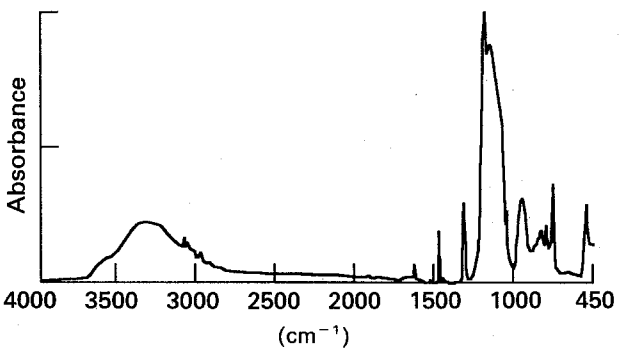

Figure 1 Typical infrared spectrum of polyphenylmethylsilsesquioxane.

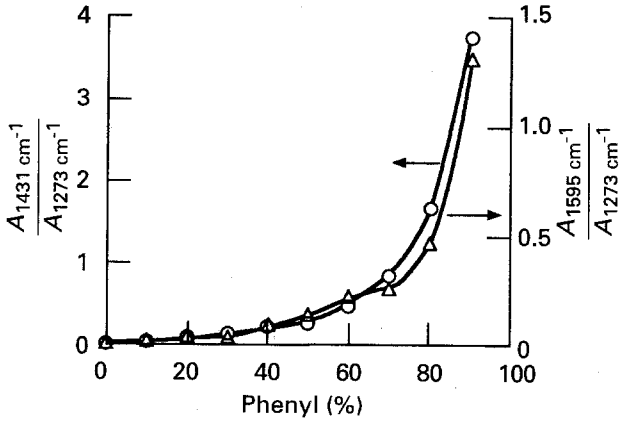

Figure 2 Ratio of phenyl/methyl infrared absorbance plotted as a function of phenyl content.

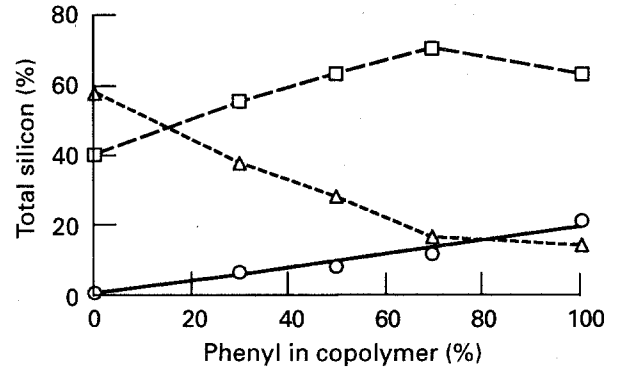

Figure 3 Structure of phenylmethylsilsesquioxane copolymers as determined by ^{29}Si NMR. (—○—) Monofunctional, (—□—) difunctional, (– –△– –) trifunctional.

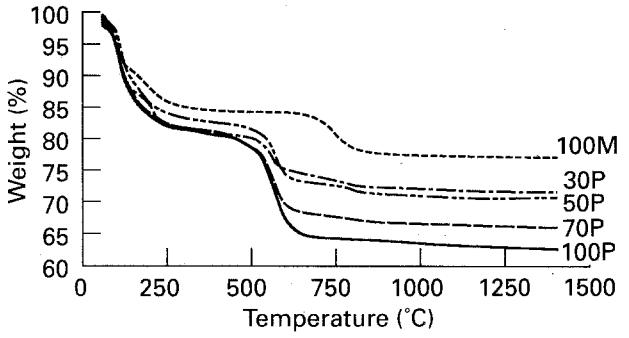

Figure 4 TGA traces of various phenylmethylsilsesquioxane copolymers heated at 10 °C min^{-1} to 1400 °C.

overlapping weight loss is observed in the region from 182–210 °C which increases in magnitude with methyl content. The derivative spectra of the methyl homopolymer actually exhibit two overlapping bands in this region centred at 182 and 207 °C (Fig. 5). Loss of siloxane is detected in this temperature range in the methyl homopolymer, and may correspond to loss of low molecular weight cyclic structures, as characterized by bands at 1020–1010 and 1090–1075 cm^{-1} in the infrared evolved gas spectrum. In contrast, only a trace of siloxane is seen in the phenyl homopolymer spectrum.

The magnitude of the weight decrease centred at 555–575 °C increases with phenyl content of the polymer, and is attributed to cleavage of benzene groups,

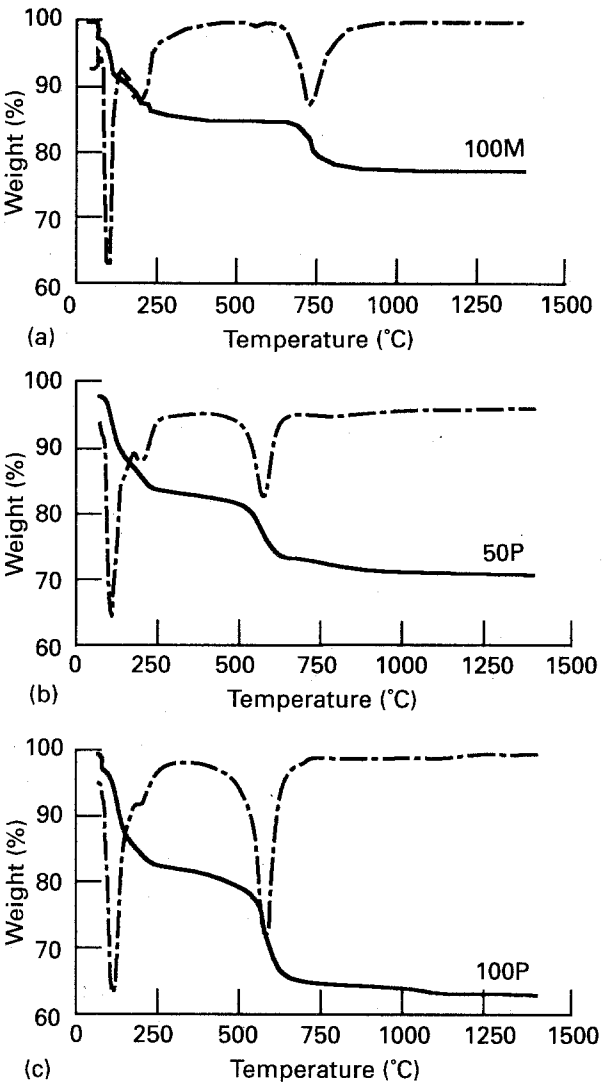

Figure 5 Comparison of weight loss curves for (a) polymethylsilsesquioxane, (b) 50 phenyl/50 methyl silsesquioxane copolymer, and (c) polyphenylsilsesquioxane. (——) Weight, (— — —) first derivative.

as characterized by the observed evolution of benzene in the infrared gas spectra. The smaller weight change at 570 °C for the methyl homopolymer corresponds to CO evolution. At 738 °C methane loss is observed in the methyl homopolymer, and to a lesser extent in the copolymers. (The TGA loss in this region is essentially proportional to the methyl concentration in the copolymer.) Between 800 and 1400 °C, weight loss is limited to $< 1.5\%$ and probably reflects evolution of hydrogen from what were $Si–CH_2–Si$ linkages incorporated into the backbone by redistribution reactions [17, 18]. Total char yields to 1400 °C ranged from 78% in the polymethylsilsesquioxane to 63% in the phenyl homopolymer. The decrease in char yield with increasing phenyl composition is consistent with decreased branching and thus a decrease in molecular weight, increasing loss of small oligomers formed by depolymerization [16], and with increased cleavage of bulky phenyl groups.

In copolymers heated just beyond 1500 °C, additional weight loss is observed, and is ascribed to evolution of CO and SiO. This conclusion is supported by the observation of both species as degradation products of the polycarbosilane-derived Nicalon

fibre [9, 10]. Performing the TGA experiment in a capped alumina crucible with a small hole at the centre of the cap, or decreasing the argon flow rate over an open alumina crucible, increases the observed weight loss. This may be due to containment of SiO long enough to allow reaction with the sample and further carbothermal reduction [19].

Elemental analysis of the chars following pyrolysis to 1400 °C in flowing argon, with a 30 min hold at the final temperature, shows that carbon content increases non-linearly with phenyl concentration in the copolymers (Fig. 6). Composition ranges from 46–30 wt % Si, 14–45 wt % C and 38–24 wt % O with increasing phenyl content. All samples showed hydrogen concentrations of $< 0.5\%$, the detection limit of the analysis.

The pyrolysis process has also been followed by solid-state ^{29}Si and ^{13}C NMR. The change in appearance of the ^{29}Si spectra of the 50P/50M copolymer pyrolysed to final temperatures of 800, 1000, 1200 and 1400 °C, is shown in Fig. 7. At 800 °C, the predominant species present is $SiCO_{3/2}$, with a peak at -64 p.p.m. $SiO_{4/2}$ at -104 p.p.m. and a smaller $SiC_2O_{2/2}$ peak at -31 p.p.m. are also evident, and likely arise from redistribution reactions [17]. The remaining possible oxycarbide species, SiC_3O, is not present in any substantial concentration. As the pyrolysis temperature is increased, the relative intensities of these three peaks shift, so that at 1000 °C the $SiO_{4/2}$ species predominates, followed by $SiCO_{3/2}$ and $SiC_2O_{2/2}$. By 1200 °C the silica peak has increased in relative intensity. At 1400 °C the oxycarbide species almost have disappeared, and a new peak at -12 p.p.m., characteristic of Si–C bonding, is observed. Comparison of the TGA studies (above) with the NMR results shows that this shift in structure is occurring over a region where there is little weight change, thus suggesting a structural reorganization rather than a major compositional change is taking place. The results presented here are in good agreement with the findings reported by others for polymethylsilsesquioxanes [13, 18], with the exception of those for oxycarbides produced from silicone resins reported by Renlund *et al.* [14, 15]. We observe only minor Si–C formation, seen as a shoulder on the $SiC_2O_{2/2}$, whereas more extensive Si–C bonding in the 1200 °C pyrolysis product is evident in Renlund *et al.*'s SR 350 derived oxycarbides pyrolysed to the same temperature [15].

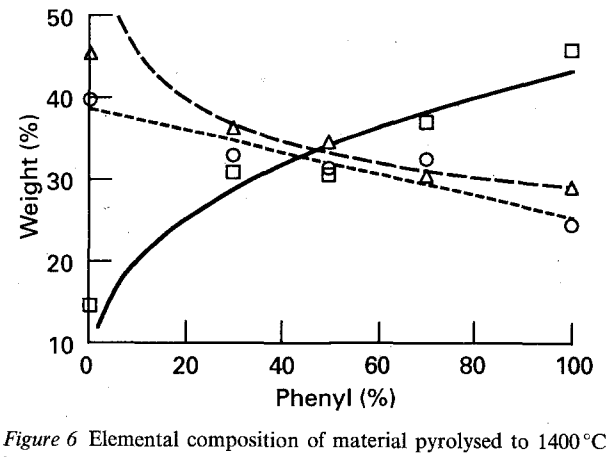

Figure 6 Elemental composition of material pyrolysed to 1400 °C in argon as a function of copolymer composition. (—□—) C, (—△—) Si, (– –○– –) O (difference).

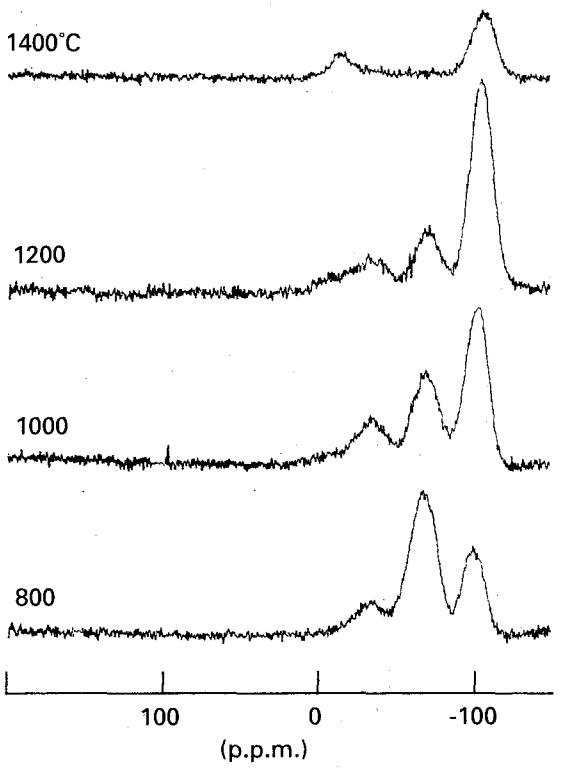

Figure 7. ^{29}Si NMR spectra of 50 phenyl/50 methyl silsesquioxane copolymer pyrolysed to 800, 1000, 1200 and 1400 °C.

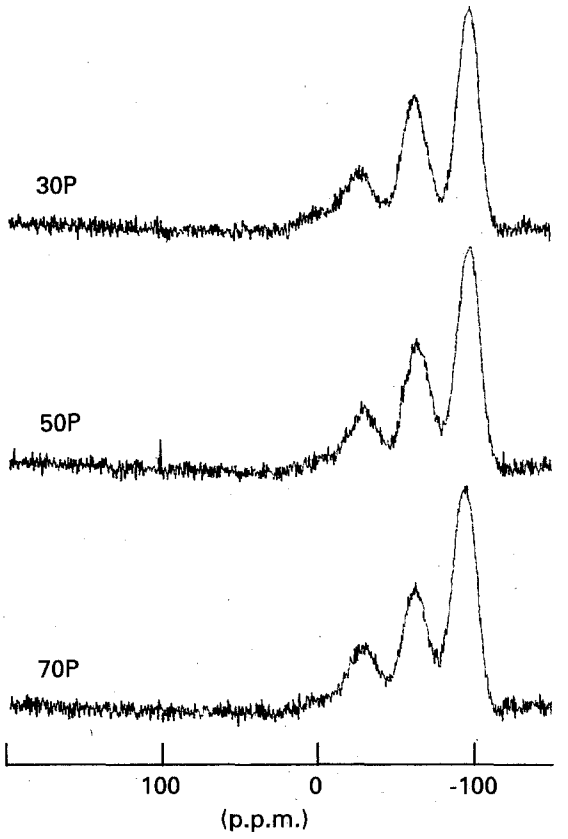

Figure 8 ^{29}Si NMR spectra of 30 phenyl/70 methyl, 50 phenyl/50 methyl and 70 phenyl/30 methyl copolymers pyrolysed to 1000 °C.

Comparison of the ^{29}Si solid-state NMR spectra for the 30P/50M, 50P/50M and 70P/30M materials pyrolysed to 1000 and 1400 °C is shown in Figs 8 and 9.

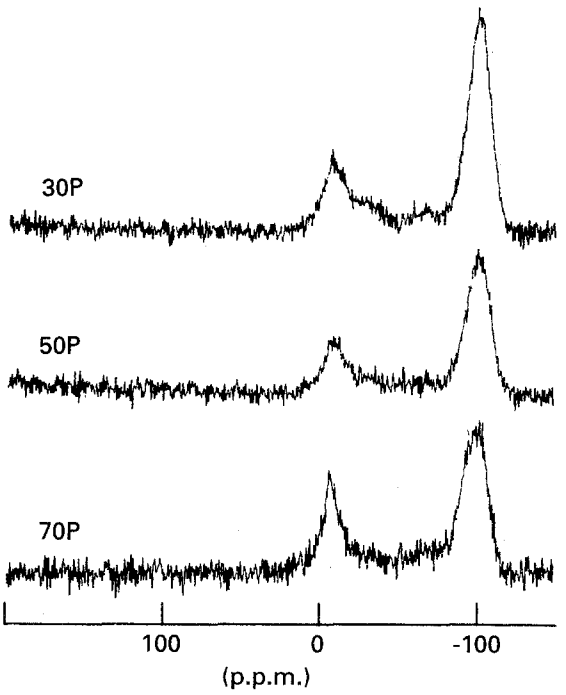

Figure 9 ^{29}Si NMR spectra of 30 phenyl/70 methyl, 50 phenyl/50 methyl and 70 phenvl/30 methyl copolymers pyrolysed to 1400 °C.

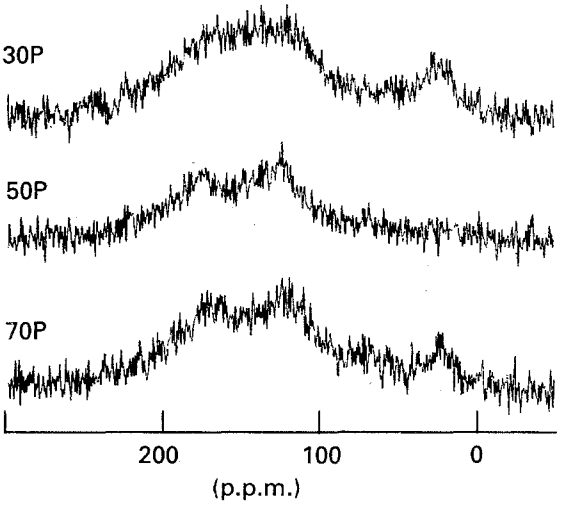

Figure 10 ^{13}C NMR spectra of 30 phenyl/70 methyl, 50 phenyl/50 methyl and 70 phenyl/30 methyl copolymers pyrolysed to 1000 °C.

At 1000 °C the relative ratios of $SiO_{4/2}$, $SiCO_{3/2}$ and $SiC_2O_{2/2}$ appear to be independent of the starting copolymer. The materials pyrolysed to 1400 °C all show two peaks characteristic of $SiO_{4/2}$ and Si–C. The relative quantity of Si–C bonds is roughly equivalent for the 30P/70M and 50P/50M products, but increases substantially for the 70P/30M composition.

The ^{13}C spectra of materials pyrolysed to 1000 °C exhibit a peak at 122 p.p.m., characteristic of sp^3 hybridized carbon. Spectra of all three copolymers are similar. At 1400 °C, the appearance of the ^{13}C spectra has changed considerably (Fig. 10), and are characterized by peaks at nominally 120 and 150–170 p.p.m., attributable to sp^3 and sp^2 carbons, respectively. A peak at 17–20 p.p.m., characteristic of SiC, is also seen in some of the samples. Si–C bonding appears minimal in the 50P/50M sample, but clearly is present in the ^{29}Si spectrum, and may be masked by the high noise level of the ^{13}C spectrum.

Raman spectroscopy was used to analyse more accurately free carbon in these materials. Samples with various starting compositions (30P/70M, 50P/50M and 70P/30M) were prepared by pyrolysis at 1000 and 1400 °C in flowing argon. The Raman spectra of all the silicon oxycarbide materials in this study are dominated by scattering from carbon [15], as can be seen by the two dominant strong bands in Figs 11 and 12. Graphite, the thermodynamically stable form of carbon at room temperature, has one symmetry-allowed E_{2g} mode at 1580 cm^{-1} and another commonly observed band at 1354 cm^{-1}. The 1354 cm^{-1} mode is due to an inplane zone-edge phonon that is symmetry forbidden for one-phonon Raman scattering. However, when the graphite crystallite size is small enough, the wavevector conservation selection rule applicable to large crystals is relaxed and Raman scattering from this phonon is observed [20].

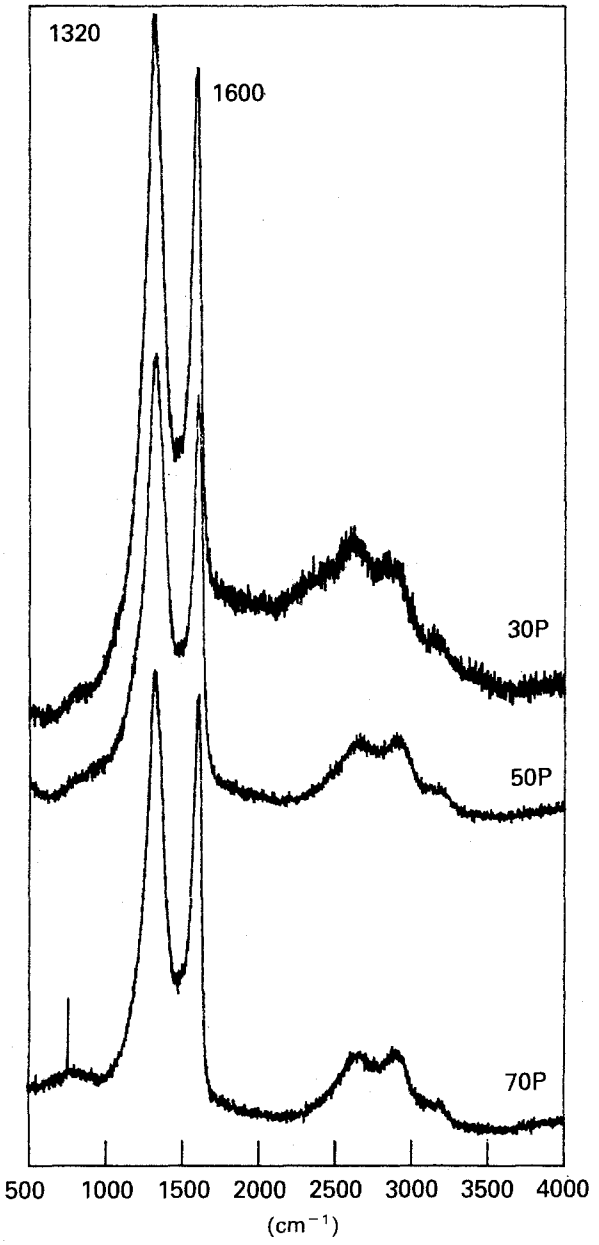

Figure 11 Raman spectra of 30 phenyl/70 methyl, 50 phenyl/50 methyl and 70 phenyl/30 methyl copolymers pyrolysed to 1000 °C.

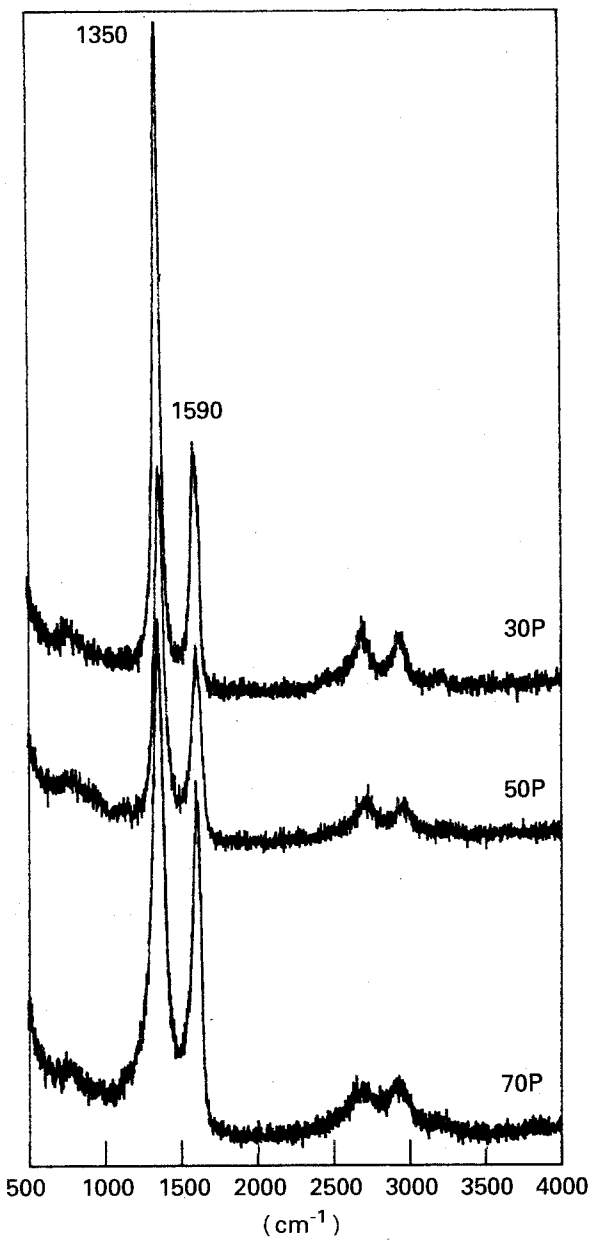

Figure 12 Raman spectra of 30 phenyl/70 methyl, 50 phenyl/50 methyl and 70 phenyl/30 methyl copolymers pyrolysed to 1400 °C.

Differences in the Raman spectra for each material are more strongly correlated with processing temperature than with starting composition. All of the silicon oxycarbides processed at 1000 °C have a band at approximately 1320 cm^{-1}, a relatively large shift from the normal carbon A_{1g} band that appears around 1354 cm^{-1}. A dramatic shift of this mode to frequencies well below that of diamond (1332 cm^{-1}) is strong evidence for sp^3 bonded carbon. Crystalline diamond, which has pure sp^3 bonding, has a broad peak in its one-phonon density of states at approximately 1300 cm^{-1}. Amorphous sp^3 carbon should have significant intensity in this spectral region [21].

The shift in frequency above 1600 cm^{-1} from the normal position at 1580 cm^{-1} for the materials processed at 1000 °C is another manifestation of the relaxation of the wavevector conservation selection rule due to crystallite size effects or defects. Contributions to Raman scattering from phonons near the peak in the one-phonon density of states just below the zone-boundary phonon at 1620 cm^{-1} (forbidden in Raman scattering from large, single-crystal graphite) cause an apparent shift to higher frequency for the 1580 cm^{-1} mode [22, 23].

In all of the materials processed to 1400 °C, the Raman bands appear very near the frequencies characteristic of sp^2-bonded carbon [23], as shown in Fig. 12. These Raman results are consistent with conversion to disordered graphite (the spectra are typical of glassy carbon) at the higher processing temperature. The Raman spectra at this temperature are similar to those reported for Nicalon fibre heated beyond 1400 °C [24], and for the pyrolysis of polycarbosilane [8]. Findings of a shift from sp^3 to sp^2 carbon with increasing pyrolysis temperature are totally consistent with the NMR evidence presented above.

The Raman spectra (Figs 11 and 12) provide no evidence for crystalline silicon carbide in any of these samples (cf. X-ray diffraction results, below). Strong Raman scattering in the 760–798 cm^{-1} region (TO phonons) and around 970 cm^{-1} (LO phonons) would be expected from any of the silicon carbide polytypes [25]. In addition, none of the crystalline forms of silica, in particular crystobalite [15], was detected by Raman spectroscopy. The broad, weak bands in both Figs 11 and 12 below 1200 cm^{-1} are probably attributable to amorphous SiO_2, with some contribution from the spectrometer optics.

Further evidence for the presence of several different forms of carbon in the pyrolysed material can be obtained by reheating samples pyrolysed in flowing argon to 1400 °C in air. If bulk material is exposed to air, silica is observed to form at the surface, with minimal weight change [26]. However, if the material is finely ground, and then heated in a TGA, two overlapping weight loss regions are observed (Fig. 13), centred at 644 and 755 °C in the 50P/50M and 70P/30M materials, suggesting two oxidation mechanisms. In the 30P/70M sample, these weight losses are shifted to higher temperatures and broaden considerably. The largest weight loss (nominally 25%) is observed for the 70P/30M product, whereas the 50P/50M and 30P/70M both retain approximately 80% of their original weight. Finely ground samples heated in air in a DTA (Fig. 14) similarly show two very broad peaks corresponding with the observed weight losses, suggesting that two different oxidation reactions are occurring. The lower temperature peak is absent in the 30P/70M sample, but sharpens and increases in magnitude with carbon content for the 50P/50M and 70P/30M materials. It is likely that this peak corresponds to oxidation of free carbon, while the higher temperature peak reflects oxidation of carbon in an Si–C network [27]. The 30P/70M sample shows a much broader peak at nominally 820 °C, and a new, smaller peak appearing at about 1000 °C. Materials remained X-ray amorphous following heating to 1000 °C in air, ruling out crystallization as the source of the DTA bands. In addition, parallel DTA experiments in argon did not reveal any changes in the samples below 1400 °C.

Copolymers pyrolysed to 1200 °C are X-ray amorphous. On pyrolysis to 1400 °C, small, broad SiC peaks are observed at 0.251 and 0.154 nm, as well as a

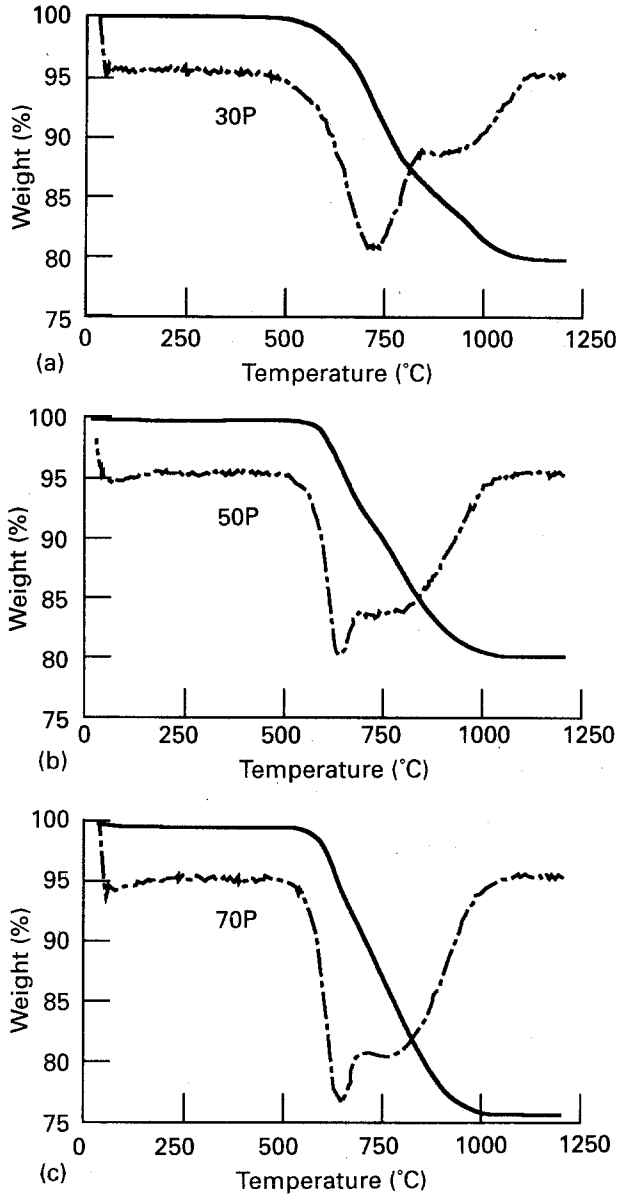

Figure 13 TGA traces obtained in flowing air of finely ground samples of materials pyrolysed in argon to 1400 °C. (a) 30 phenyl/70 methyl, (b) 50 phenyl/50 methyl, (c) 70 phenyl/30 methyl. (——) Weight, (– – –) first derivative.

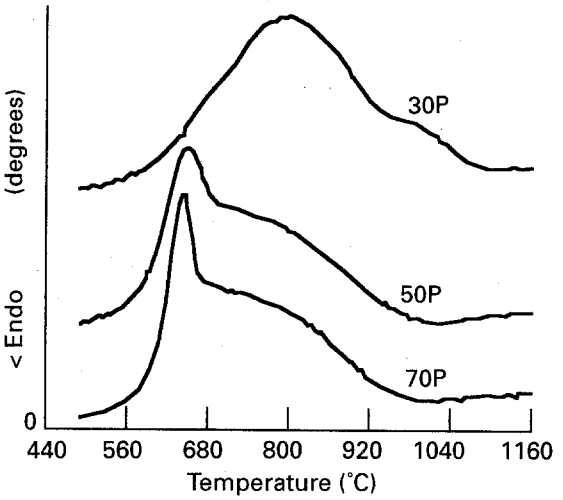

Figure 14 DTA traces obtained in flowing air of finely ground samples of materials pyrolysed in argon to 1400 °C.

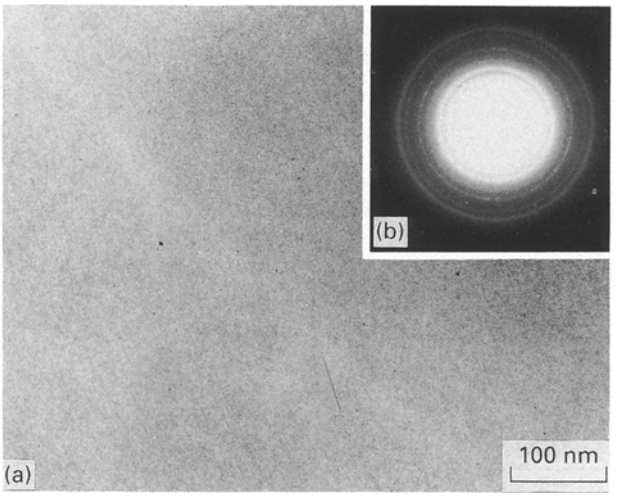

Figure 15 (a) Bright-field TEM image of 70 phenyl/30 methyl copolymer pyrolysed to 1400 °C in argon showing fine-scale phase separation. (b) Spotty diffraction rings obtained in selected-area X-ray diffraction are indicative of small crystalline SiC and C.

small C peak at 0.209 nm. Examination of copolymers with compositions of 30P/70M, 50P/50M and 70P/30M showed this small carbon peak to be most evident in the higher carbon-containing (70P/30M-derived) material.

Transmission electron microscopy can be used effectively to assess crystallinity as well as homogeneity and phase distribution in pyrolysed polymers. The techniques employed are bright-field imaging, dark-field imaging and selected-area diffraction. Detailed phase analysis procedures in Si–O–C systems have been presented by Ayache *et al.* [28] and others [3, 29, 30]. Such procedures were followed here in the examination of the 30P/70M, 50P/50M and 70P/30M materials pyrolysed to 1400 °C in argon. Two different sample forms were used. Ion milling examines the bulk material, whereas crush–mount techniques capture both the surface and bulk materials, and should be complementary to the results obtained by X-ray diffraction.

Bright-field images of ion-milled specimens have a mottled contrast indicative of fine-scale phase separation in all three materials (Fig. 15a). Diffraction rings for crystalline SiC {(1 1 1), (2 2 0), (2 2 2) and (3 1 1) spacings}, a broad, strong ring about the (0 0 2) carbon spacing, and weaker (1 0 1) and (0 0 4) carbon rings were obtained in selected-area diffraction patterns (Fig. 15b). There is no unambiguous diffraction evidence for crystalline SiO_2. SiC diffraction rings in 30P/70M and 70P/30M exhibited discrete maxima superimposed on the SiC rings indicative of a larger crystal size.

This larger crystallite size was confirmed in dark-field images. SiC crystals were imaged in dark-field using (2 2 0) SiC diffracted intensity. The crystal size was smallest in 50P/50M material: nominally 2–3 nm. 30P/70M material contained SiC crystals of 2–10 nm diameter. SiC in 70P/30M material ranged from 2–30 nm in size, with the majority of particles < 8 nm. Dark-field images obtained with the aperture centred about (0 0 2) carbon diffracted intensity revealed a particle size of approximately 2 nm in all specimens. A contribution to these images from

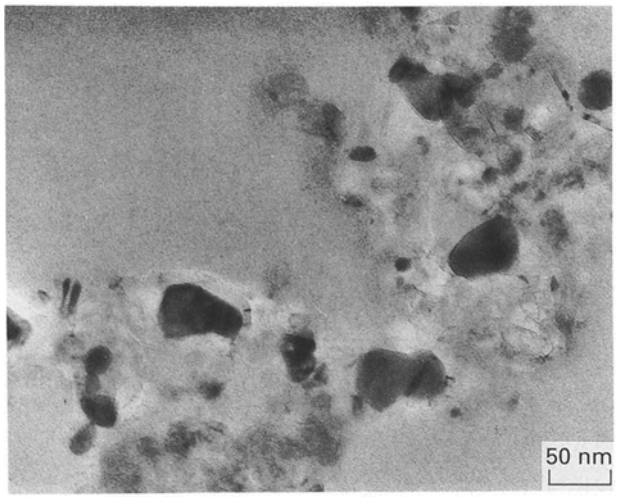

Figure 16 Crush–mount preparation shows large crystallites of SiC surrounded by fibrous carbon obtained in 70 phenyl/30 methyl material pyrolysed to 1400 °C material in argon.

amorphous SiO_2 cannot be excluded and would be evinced as weak bright spots about the size of the image resolution of about 1 nm [28]. No preferred orientation of phases was noted in the ion-milled specimens.

Crush–mount specimens also were examined. Material was ground and suspended on carbon grids. Such samples contained much larger SiC crystals than those seen in the ion-milled specimens, and are assumed to have been contributed by surface material which is lost on ion milling. SiC particles up to 70 nm in size, and surrounded by fibrous carbon, were observed (Fig. 16). The imaging of an ordered carbon supports the observation of graphite-like carbon in the Raman (see Fig. 12).

The greater homogeneity of the 50P/50M sample may arise from a more random distribution of phenyl groups in the 50/50 copolymer, and hence a more uniform distribution of carbon in the pyrolysed material which suppresses crystallization.

4. Conclusions

The current work indicates that copolymer composition of polysilsesquioxanes, in which one of the monomers contains a phenyl substituent, can be used to control the elemental composition of the amorphous materials which result on pyrolysis. By controlling the carbon content, both the modulus and coefficient of thermal expansion of these materials should be able to be tailored.

Characterization of the conversion process established the formation of oxycarbides, evident on pyrolysis to 800 °C. Over the 30–70 mol % phenyl range studied, ratios of the various oxycarbides formed does not vary with carbon content; rather, additional carbon is present as free carbon. Significant oxycarbide structure is maintained to 1200 °C under inert conditions. Between 1200 and 1400 °C this oxycarbide configuration is lost, primarily through structural rearrangement (there is minimal loss of weight). At 1000 °C the free carbon is present as glassy carbon; at 1400 °C, it is evident as disordered graphite.

Based on the presence of Si–C bonds in the 1400 °C materials as observed by solid-state NMR, the absence of crystalline SiC peaks in the Raman, the appearance of small, broad SiC peaks by diffraction and TEM evidence of microcrystalline SiC and spotty rings in selected-area X-ray diffraction, we can conclude that SiC bonding exists primarily as an amorphous network, as has been proposed for SiC ceramics derived from polycarbosilane [27].

The presence of carbon acts to inhibit the crystallization of silica. Despite the large $SiO_{4/2}$ peak which characterizes the ^{29}Si NMR spectra, none of the crystalline forms of silica are observed by Raman, X-ray diffraction or TEM.

Oxidation studies of finely ground samples (TGA, DTA) indicate at least two distinct oxidation processes, with oxidation occurring much more slowly at the lowest carbon composition (30P/70M).

Finally, polysilsesquioxanes can serve as easily synthesized precursors to silicon oxycarbides which persist to temperatures of at least 1200 °C. Between 1200 and 1400 °C the oxycarbide structure is lost, but the resulting amorphous materials remain thermally stable. Significant carbothermal reduction (and weight loss) are not observed until > 1500 °C. The use of phenyl-containing monomers to introduce finely dispersed free carbon could be useful for tailoring modulus and thermal expansion of the final products, and, if the carbon is totally isolated from the surface, oxidative stability may not necessarily be compromised. Lower phenyl concentrations need to be explored to determine the minimum carbon concentration required for processability and suppression of crystallization of silica, while maintaining other desired physical and mechanical properties. These systems offer promise for a variety of applications, including matrices, infiltrants and coatings in ceramic matrix composites.

Acknowledgements

The authors thank Terrance A. Kacik, Ruth E. Cipcic and Cheol J. Kim for technical assistance, and Dr David Harding for helpful discussions.

References

1. J. HOMENY, G. G. NELSON and S. H. RISBUD, *J. Am. Ceram. Soc.* **71** (1988) 386.
2. R. PAMPUCH, W. PTAK, S. JONAS and J. STOCH, *Mater. Sci. Monographs* **6** (1990) 435.
3. E. BOUILLON, D. MOCAER, J. F. VILLENEUVE, R. PAILLER, R. NASLAIN, M. MONTHIOUX, A. OBERLIN, C. GUIMON and G. PFISTER, *J. Mater. Sci.* **26** (1991) 1517.
4. E. BOUILLON, R. PAILLER, R. NASLAIN, E. BACQUE, J.-P. PILLOT, M. BIROT, J. DUNOGUES and P. V. HUONG, *Chem. Mater.* **3** (1991) 356.
5. F. BABONNEAU, G. D. SORARU and J. D. MACKENZIE, *J. Mater. Sci.* **25** (1990) 3664.
6. J. LIPOWITZ, *Ceram. Bull.* **70** (1991) 1888.
7. L. PORTE and A. SARTRE, *J. Mater. Sci.* **24** (1989) 271.
8. E. BOUILLON, F. LANGLAIS, R. PAILLER, R. NASLAIN, F. CRUEGE, P. V. HUONG, J. C. SARTHOU, A. DELPUECH, C. LAFFON, P. LAGARDE, M. MONTHIOUX and A. OBERLIN, *ibid.* **26** (1991) 1333.

9. Y. SASAKI, Y. NISHINA, M. SATO and K. OKAMURA, *ibid.* **22** (1987) 443.
10. S. M. JOHNSON, R. D. BRITTAIN, R. H. LAMOREAUX and D. J. ROWCLIFFE, *J. Am. Ceram. Soc.* **71** (1988) C132.
11. L. C. SAWYER, R. T. CHEN, F. HAIMBACH IV, P. J. HARGET, E. R. PRACK and M. JAFFE, *Ceram. Eng. Soc. Proc.* **7** (1986) 914.
12. F. BABONNEAU, K. THORNE and J. D. MACKENZIE, *Chem. Mater.* **1** (1989) 554.
13. H. ZHANG and C. G. PANTANO, *J. Am. Ceram. Soc.* **73** (1990) 958.
14. G. M. RENLUND, S. PROCHAZKA and R. H. DOREMUS, *J. Mater. Res.* **6** (1991) 2716.
15. *Idem., ibid.* **6** (1991) 2723.
16. P. J. HEIMANN, F. I. HURWITZ and A. L. RIVERA, *Ceram. Trans.* **19** (1991) 27.
17. V. BELOT, R. J. P. CORRIU, D. LECLERCQ, P. H. MUTIN and A. VIOUX, *J. Mater. Sci. Lett.* **9** (1990) 1052.
18. R. M. LAINE, J. A. RAHN, K. A. YOUNGDAHL, F. BABONNEAU, M. L. HOPPE, Z.-F. ZHANG and J. F. HARROD, *Chem. Mater.* **2** (1990) 464.
19. J. J. BIERNACKI and G. P. WOTZAK, *J. Am. Ceram. Soc.* **72** (1989) 122.
20. F. TUINSTRA and J. L. KOENIG, *J. Chem. Phys.* **53** (1970) 1126.
21. N. WADA, P. J. GACZI and S. A. SOLIN, *J. Non-Cryst. Solids* **35–36** (1980) 543.
22. D. S. KNIGHT and W. B. WHITE, *J. Mater. Res.* **4** (1989) 385.
23. R. J. NEMANICH and S. A. SOLIN, *Phys. Rev. B* **20** (1979) 392.
24. R. J. DAY, V. PIDDOCK, R. TAYLOR, R. J. YOUNG and M. ZAKIKHANI, *J. Mater. Sci.* **24** (1989) 2898.
25. D. W. FELDMAN, J. H. PARKER Jr, W. J. CHOYKE and L. PATRICK, *Phys. Rev.* **173** (1968) 787.
26. F. I. HURWITZ, J. Z. GYEKENYESI, P. J. CONROY and A. L. RIVERA, *Ceram. Eng. Sci. Proc.* **11** (1990) 931.
27. G. D. SORARU, F. BABONNEAU and J. D. MACKENZIE, *J. Mater. Sci.* **25** (1990) 3886.
28. J. AYACHE, S. BONNAMY, X. BOURRAT, A. DEURBERGUE, Y. MANIETTE, A. OBERLIN, E. BARQUE, M. BIROT, J. DUNOGUES and J.-P. PILLOT, *J. Mater. Sci. Lett.* **7** (1988) 885.
29. Y. MANIETTE and A. OBERLIN, *J. Mater. Sci.* **24** (1989) 3361.
30. *Idem., ibid.* **25** (1990) 3864.

Received 28 July 1992
and accepted 7 May 1993